Journal of Neonatal Surgery
ISSN (Online): 2226 -0439
Vol. 14, Issue 29s (2025)
https://www.jneonatalsurg.com

OPEN ACCESS

Identifying The Nssnps (Non-Synonymous Snps) Of Gene (SLC11A1) Involved In Spinal Tuberculosis

Shubhra Sharma[1], Amaresh Mishra[2], Rajan Kumar Singh[2*], Amresh Prakash[1*]

[1]Data Science Lab, Amity Institute of Integrative Sciences and Health, Amity University, Haryana, Gurugram-122413, India

[2]Department of Biotechnology Engineering, Parul University, Vadodara-391760, India

***Corresponding Authors:**

Dr. Amresh Prakash[1*], Dr. Rajan Kumar Singh[2*]

[1*]Data Science Lab, Amity Institute of Integrative Sciences and Health, Amity University, Haryana, Gurugram-122413, India,

Email ID: aprakash@ggn.amity.edu

[2*]Department of Biotechnology, Parul Institute of Technology, Faculty of Engineering and Technology, Parul University, Vadodara - 391760

Email ID: rajankumar.singh22658@paruluniversity.ac.in

Cite this paper as: Shubhra Sharma, Amaresh Mishra, Rajan Kumar Singh, Amresh Prakash, (2025) Identifying The Nssnps (Non-Synonymous Snps) Of Gene (SLC11A1) Involved In Spinal Tuberculosis. *Journal of Neonatal Surgery*, 14 (29s), 921-938.

Graphical Abstract

Prediction Analysis of nsSNPs

Homology Modeling

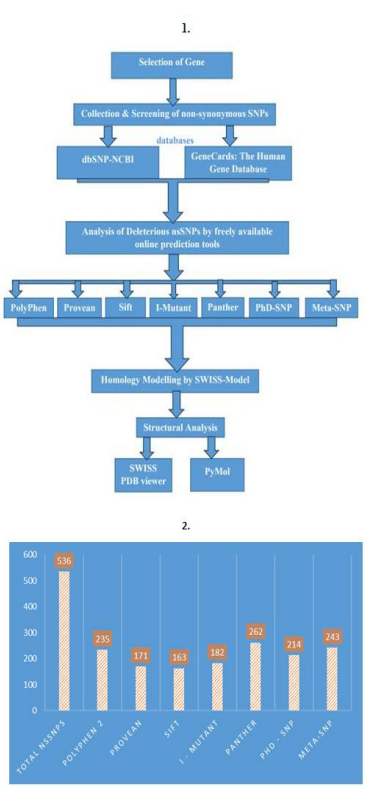

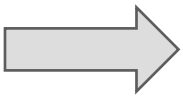

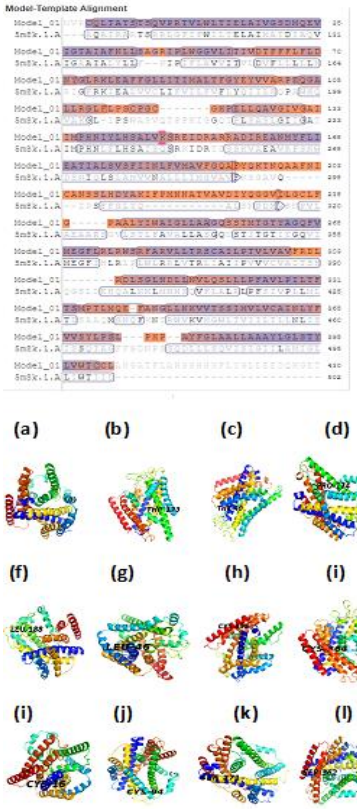

Ligand Binding Site Protein

Superimposition of Wild-Type with Mutant Model

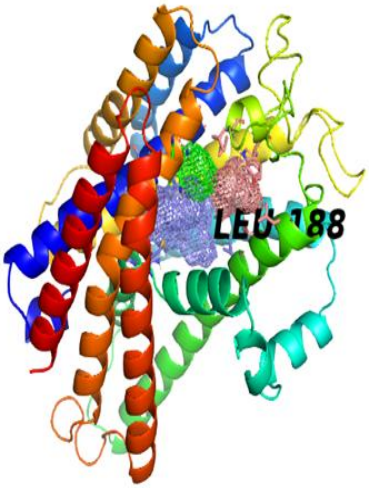

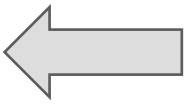

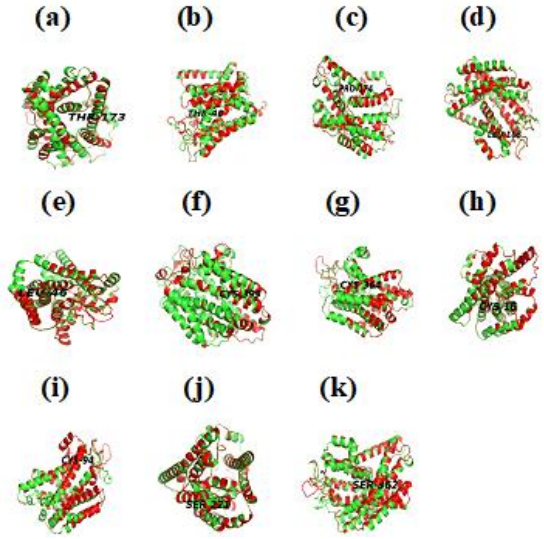

ABSTRACT

Introduction: Single Nucleotide Polymorphisms (SNPs) play a vital role in understanding the genetic basis for several complicated human diseases. Additionally, knowing the functions of these SNPs might help us understand the genetics of human trait diversity. Identifying functional SNPs in a disease-related gene remains a major challenge. In this study, we have applied computational approaches to examine the genetic variation that can affect the SLC11A1 gene's expression and functionality. There were 7243 SNPs in all, 536 of them were missense/non-synonymous SNPs. **Methods**: We have employed a comprehensive analysis of the effect of all nsSNPs in the SLC11A1 gene using numerous methods like PolyPhen-2, PROVEAN, SIFT, I-Mutant, PANTHER, PhD-SNP, and Meta-SNP. The PolyPhen-2 identified 235 nsSNPs

as probably damaging. PROVEAN shows 171 as deleterious nsSNPs. SIFT defines 163 nsSNPs as deleterious. I-Mutant has predicted 182 nsSNPs having decreased/increased stability. PANTHER found 262 nsSNPs as probably damaging, whereas PhD-SNP and Meta-SNP showed 214 and 243 as disease-associated mutations. **Results:** Comparing the predicted results from all these 7 methods, 11 nsSNPs rs139480250(Ala173Thr), rs141932707(IIe40Thr), rs145536242(Leu174Pro), rs150192588(Phe188Leu), rs151164925(Ser46Leu), rs182057473(Tyr395Cys), rs182057473(Tyr364Cys), rs201910426(Arg16Cys), rs367630718(Tyr94Cys), rs375775521(Gly271Ser), rs377166486(Asn362Ser) were found to be harmful. The study suggests the deleterious efficiency of these 11 nsSNPs in the SLC11A1 gene, which needs to be explored in relation to Spinal Tuberculosis. However, homology modeling and structural analysis were performed on previously empirically verified nsSNPs to ensure the predictability of projected models. The mutant models had higher energy and Root mean square deviation (RMSD) scores. Furthermore, FT-Site predicted one nsSNP, rs150192588(Phe188Leu) at the first binding region of the NRAMP1 protein out of the 11 picked-up nsSNPs. STRING predicted the functional interaction of the NRAMP1 protein. **Conclusions:** As a result of the current computational analysis, anticipated nsSNP may be a better pharmacological target contributing to treating and understanding spinal tuberculosis.

Keywords: *SLC11A1; NRAMP1; Spinal Tuberculosis; SNPs; Homology modeling; FT-Site; STRING*

1. INTRODUCTION

Tuberculosis (TB) is caused by Mycobacterium tuberculosis infection and is one of the leading causes of death worldwide. It has infected more than one-third of the world's population, but only 10% have developed clinical TB(Jin et al., 2009). Nearly 2 billion people are thought to be infected with latent Mycobacterium tuberculosis (Mtb). According to the World Health Organization's 2020 Global Tuberculosis Report, TB is still a serious public health issue, claiming nearly 1.4 million deaths worldwide in 2019 (Organization, 2020). Infections of TB are typically found in the lungs. Although multidrug-resistant tuberculosis is uncommon in spinal disease, a few case reports have emerged in recent years(Garg and Somvanshi, 2011). Out of 729 tuberculosis patients in 2004 approximately 8% of the cases were found to have musculoskeletal involvement, with nearly 50% of these patients having spinal involvement. In most parts of the world, the exact incidence and prevalence of spinal tuberculosis are unknown. The incidence is expected to be comparatively high in countries with a high burden of pulmonary tuberculosis. Approximately 10% of patients with extrapulmonary tuberculosis have skeletal involvement. The spine is usually the most affected skeletal site, followed by the hip and knee. Spinal tuberculosis (STB) is also called Pott’s disease, the most prevalent and potentially fatal type of skeletal TB(Rasouli et al., 2012). It accounts for approximately half of all musculoskeletal tuberculosis cases. It is more prevalent in teenagers and children(Garg and Somvanshi, 2011). The incidence of STB is rising in developed countries. It is responsible for 50−75% of STB cases and nearly 4% of all TB cases(Li et al., 2022). STB, which leads to vertebral bone degeneration, collapse, and fractures, causes far more destruction and death at a high rate compared to other bone TB and pulmonary TB and is a major cause of disability as well as death rates. Fortunately, it was expected that only 10% of individuals were infected with Mtb acquire TB, highlighting the role of genetic susceptibility in the development of TB(Li et al., 2022).

Recent studies have proven that innate immunity including the SLC11A1 gene, is strongly linked to Mtb infection and TB pathogenesis. However, polymorphisms of genes affecting the innate immune response play an important role in TB susceptibility and development(Li et al., 2022). The SLC11A1 i.e., solute carrier family 11 proton-coupled divalent metal ion transporter membrane1 (formerly known as NRAMP1, natural resistance-associated macrophage protein) has been the most extensively investigated main candidate gene associated with TB susceptibility(Jin et al., 2009). It plays a major role in the development of immunological responses in TB. The protein function as a divalent transition metal (iron and manganese) transporter that is involved in the lysosomal membrane(Patel et al., 2015). Furthermore, iron is an essential mycobacterial nutrient and plays an important role in the production of reactive oxygen as well as nitrogen compounds in macrophages(Amiri et al., n.d.). Several studies confirmed that NRAMP1 has been involved in many different types of inflammatory and infectious disorders. *R Bellamy et al.* in 1998 employed sequence-defined oligonucleotide crossover and microsatellite evaluation to identify SLC11A1 mutations in 410 stain-positive TB patients along with 417 run-matched healthy volunteers, illustrating that four mutations occurred in the SLC11A1 gene, 3′ untranslated region(3'UTR), 5'(CA)n, D543N, and intron 4(INT4). Each was found to be significantly linked with the disease, and *Bellamy et al.* (1998) were the first to discover that SLC11A1 variations alter susceptibility to tuberculosis in West Africans. *Wu et al.* (2013) performed a case-control research study and found that NRAMP1 gene polymorphisms are strongly linked with TB susceptibility in China's Kazakh community(Li et al., 2022).

However, SNPs, also known as Single Nucleotide Polymorphisms, are the most common form of genetic mutation in humans. Approximately 93% of all human genes have been reported to have at least one SNP(Alam et al., n.d.). They play an important role in understanding the genetic basis of many complex diseases, but identifying functional SNPs in disease-related genes remains a major challenge. Understanding how these genetic variants affect phenotypes could therefore be an initial step in determining the cause of many disorders and diseases. SNPs can occur in the intergenic

region between two genes, in the coding or non-coding regions of genes(Datta et al., 2015). Although coding and non-coding SNPs have no phenotypic effects, nsSNPs are thought to have an impact on phenotype by changing the protein sequence. SNPs are also markers that can be used to identify the region of the genome that is connected to a particular disease. Non-synonymous coding SNPs (nsSNPs) are thought to alter the protein sequence, which has a significant effect on phenotype. As they change the amino acids in correspondence to protein products, it may exert negative effects on the function, structure, solubility, or stability of proteins(Datta et al., 2015). Besides, these non-synonymous SNPs also change the gene regulation by altering DNA and transcriptional binding factors(Rajasekaran et al., 2007). It also maintains the structural integrity of cells and tissues (Datta et al., 2015). Non-synonymous SNPs (nsSNPs) significantly impact the functional diversity-coded proteins in human populations, which are frequently linked to human diseases(Akhoundi et al., 2016). Furthermore, past studies have proven that more than 50 percent of the mutations linked to inherited genetic diseases result from nsSNPs(Datta et al., 2015). Thus, many studies have recently concentrated on nsSNPs in tuberculosis-causing genes. In the present study, we investigated the mutational effect of nsSNPs of the SLC11A1 gene. An extensive computational analysis results in the identification of 11 deleterious mutations that may be involved in STB.

2. MATERIALS & METHODS

2.1 Search for non-synonymous SNPs (nsSNPs) and mutations

The non-synonymous SNPs of gene SLC11A1 were taken from the NCBI database(https://www.ncbi.nlm.nih.gov/), which is further validated on Gene Cards, a human gene database (http://www.genecards.org/cgi-bin/snp). The impact of missense mutations on the structure of the protein (NRAMP1: UniProt id P49279) (http://www.uniprot.org/) was detected using PolyPhen, PROVEAN, SIFT, I-Mutant, PANTHER, PhD-SNP & Meta-SNP. The SLC11A1 encodes a protein that consists of 550 amino acids.

2.2 Functional effect of nsSNPs

Polymorphism Phenotyping-2 (PolyPhen-2) is an online program that predicts the effect of a change in amino acids on the structure and function of a human protein(Elnasri et al., 2018). Based on the PSIC (position-specific independent count) score, it classifies coding nsSNPs as possibly damaging, probably damaging, or benign (Saleh et al., 2016). PolyPhen-2 estimates the genuine positive rate as a proportion of correctly anticipated mutations for a specific threshold of naive bayes probability score.

2.3 Analysis of Deleterious Mutations

The Protein Variation Effect Analyzer (PROVEAN) is a novel tool that employs an alignment-based scoring technique. PROVEAN, unlike most other programs, can predict not only single amino acid changes but also multiple amino acid substitutions, insertions, and deletions using the same underlying scoring method. Based on the threshold, this approach provides for the best-balanced separation of deleterious and neutral amino acids(Patel et al., 2015). To determine the functional effect of nsSNPs, the PROVEAN server was given a query peptide sequence of SLC11A1 in FASTA format.

2.4 Investigation of Deleterious nsSNPs

SIFT is another sequence homology-based tool for analyzing deleterious nsSNPs. It evaluates homologous sequences using Swiss-Prot/TrEMBL. As previously stated, the program relies on multiple alignments of a wide range of peptide sequences. It estimates whether a substitution with any of the other amino acid groups is tolerated or as damaging for every single position in the uploaded sequence. It distinguishes between functionally neutral and harmful polymorphisms during human mutagenesis investigations, based on earlier published data(Hussain et al., 2012).

2.5 Identification of Protein Stability

I-Mutant 2.0 is a Support Vector Machine (SVM) based tool used to predict the stability of protein changes caused by single-site mutations(Abd Elhamid Fadlalla Elshaikh et al., 2016). The thermodynamics parameter, free energy changes in protein stability due to mutation under various conditions, was calculated in terms of DDG value (kcal/mol)(Datta et al., 2015). Further, the reliability index (RI) value was also calculated for the stability of amino acids.

2.6 Analysis Through Evolutionary Relationships

Protein Analysis Through Evolutionary Relationships (PANTHER), the very first database, is based on the Hidden Markov Model (HMM). It uses evolutionary and functional data to determine protein families with common functions and sequences. It analyses the protein's sequence to a family of evolutionarily related proteins and calculates the likelihood of harmful (Pdeleterious) nsSNPs dependent on subPSEC (substitution position-specific evolutionary conservation) value (Ali Mohamoud et al., 2014). If the subPSEC value is -3, it equates with a Pdeleterious of 0.5, and the higher the Pdeleterious, the more damaging (deleterious) the nsSNPs.

2.7 Identification of disease-causing nsSNPs

PhD-SNP (Predictor of Human Deleterious Single Nucleotide Polymorphisms) is a support vector machine (SVM) based algorithm that uses protein sequence information to determine whether an nsSNP is disease-related(Elnasri et al., 2018). The output is derived from the frequencies of wild as well as mutant residues, the number of matched sequences, and the

conservation index computed at the position involved. It predicts whether the polymorphism is illness-related (disease) or neutral, with a prediction efficiency of 78%.

2.8 Detection of disease-associated nsSNPs

Another tool, the Meta-SNP server, was also used for the prediction of disease-causing variants. It has been developed to determine the disease-associated single-point protein variation and gives 79 % accurate results.

2.9 Homology Modeling and Structural Analysis of wild-type and mutant protein

SWISS-MODEL was used to predict the three-dimensional (3D) structure of wild-type(native) NRAMP1 protein and mutants. Swiss-PDB viewer and PyMOL were applied for the structural analyses (energy minimization, RMSD) and visualization of structures (Version 1.7.4, Schrodinger, LLC). VADAR was used to calculate H-bond energy. Further to validate the predicted models, the PROCHECK server was used to analyze the stereochemical properties and Ramachandran plots.

2.10 Ligand Binding Site Prediction

FT-Site was used to identify the ligand binding regions of NRAMP1. It defines the consensus site of ligand binding using FT-Map. The molecular binding site is categorized as a hot spot, the strong "main", considering the proximal probability of a hot spot and the possibility of bonded and non-bonded interactions with probes in the consensus clusters.

2.11 Protein-protein interactions

The protein-protein interaction analysis was performed using the STRING server, which focused on the networks and interactions of proteins in many different species. The analyses include both direct "physical" and indirect "functional" interactions(Desai and Chauhan, 2019). It consists of data from the genetic context, scientific databases, and public text resources. The protein-protein interactions of NRAMP1 were investigated against the homo sapiens.

Table 1: List of computational tools used for the prediction of the NRAMP1 protein.

Server	URL	Feature/Prediction Result
Polyphen-2 (Polymorphism Phenotyping)	http://genetics.bwh.harvard.edu/pph2/	Predicts the impact of an amino acid change on the structure and function of a protein.
PROVEAN (Protein Variation Effect Analyzer)	http://provean.jcvi.org/index.php	A sequence-based prediction that evaluates whether a difference in protein sequence affects the functioning of proteins.
SIFT (Sorting Intolerant From Tolerant)	https://sift.bii.a-star.edu.sg/	Predicts the impact on the function of proteins based on sequence homology & physical characteristics of amino acids
I-Mutant 2.0	http://folding.biofold.org/cgi-bin/i-mutant 2.0	Estimates the change in stability of proteins caused by mutation.
PANTHER (Protein Analysis Through Evolutionary Relationships)	www.pantherdb.org	A database of protein families & subfamilies that estimates the frequency of the presence of amino acids at a specific position in evolutionarily related sequences of proteins.
PhD-SNP (Predictor of human Deleterious Single Nucleotide Polymorphisms)	http://snps.biofold.org/phd-snp/phd-snp	SVM (support vector machine) based on evolutionary data.
Meta-SNP server (Meta-predictor of disease-causing variants)	http://snps.biofold.org/meta-snp	Determine whether a particular single-point protein variation is disease-related or a polymorphism.
SWISS MODEL	http://swissmodel.expasy.org	An automated comparative modeling server for three-dimensional (3D) protein structures
Swiss PDB Viewer (spdbv)	https://spdbv.unil.ch/	A program with an accessible interface that allows for the evaluation of several proteins at the same time.

PyMol	https://pymol.org/dsc/	Open source for 3D macromolecule visualization.
VADAR (Volume, Area, Dihedral Angle Reporter)	http://redpoll.pharmacy.ualberta.ca/vadar	Program for analysing and evaluating peptide & protein structure.
PROCHECK	https://www.ebi.ac.uk/thornton-srv/software/PROCHECK/	A program to check the stereochemical quality of protein
FT-Site	http://ftsite.bu.edu	Predicts the ligand binding site of a particular protein
STRING (Search Tool for the Retrieval of Interacting Proteins)	https://string-db.org/	Protein-protein interaction database with known & anticipated interactions

3. RESULTS AND DISCUSSION

3.1 Prediction of nsSNPs for the SLC11A1 gene

The SLC11A1 gene of homo sapiens consists of 7243 SNPs, among them 536 are reported as missense/non-synonymous (nsSNPs), 2337 are non-coding SNPs, 770 are synonymous SNPs, 2337 are non-coding transcript variants and 6175 are introns. The extensive computational analyses for the prediction of non-synonymous SNPs involved in STB disease are illustrated in a flow chart in **Figure 1**. Herein, all 536 nsSNPs were taken for further study. The computational methods applied for analyses of nsSNPs and their efficacy are enumerated in **Table 1**. Our collective results suggest that 11 nsSNPs may be involved in STB disease (**Figure 2**).

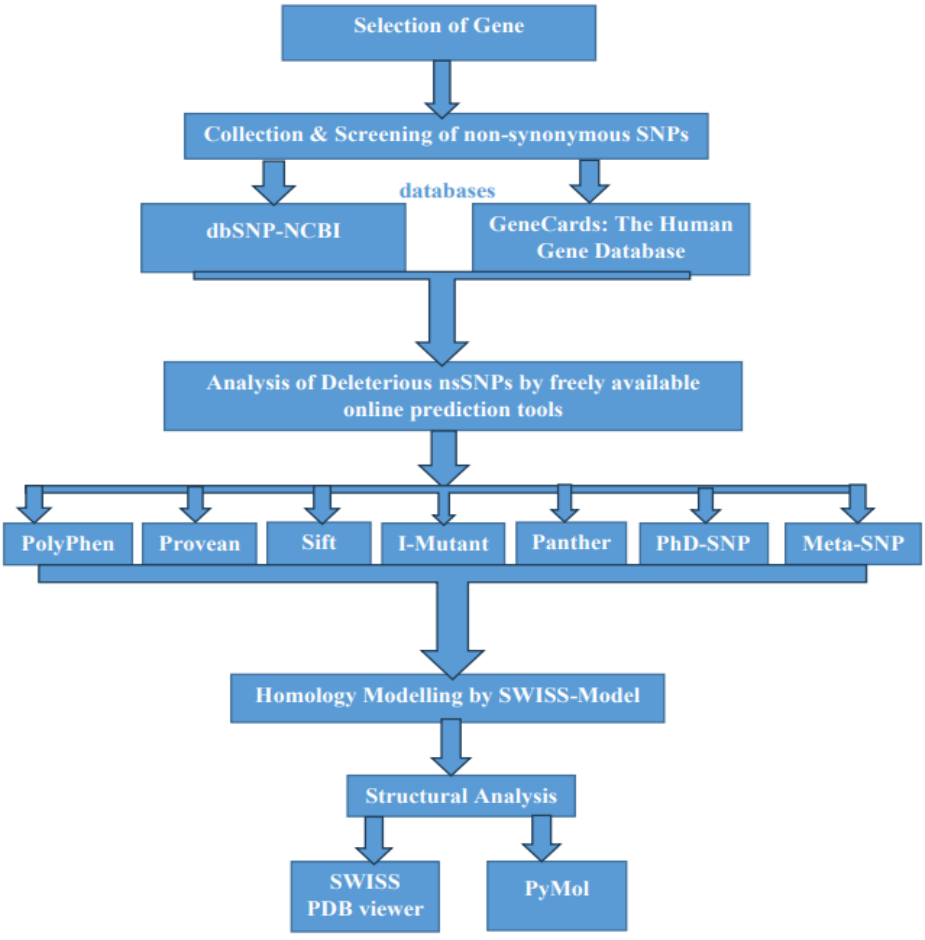

Figure 1. Flowchart of the prediction of non-synonymous SNPs (nsSNPs) belonging to the SLC11A1 gene involved in STB disease.

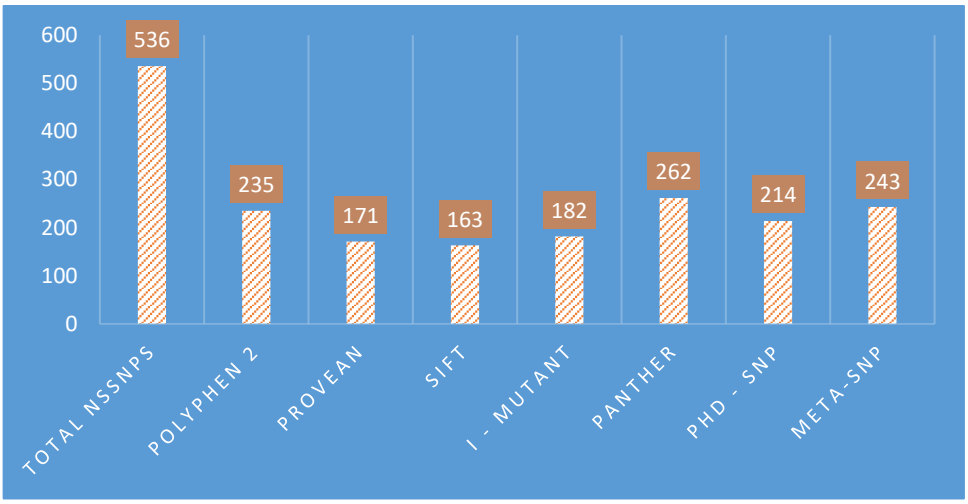

Figure 2. Prediction of deleterious non-synonymous SNPs of the SLC11A1 gene, applying the different computational methods: PolyPhen-2 predicted 235 nsSNPs as probably damaging. PROVEAN shows 171 as deleterious nsSNPs. SIFT defines 163 nsSNPs as deleterious. I-Mutant predicts 182 nsSNPs having a decrease/increase in protein stability. PANTHER predicted 262 nsSNPs as probably damaging. PhD-SNP and Meta-SNP suggested 214 and 243 as disease-based mutations.

3.2 Detection and Comparison of the functional effect of nsSNPs

To determine the functional effect of SLC11A1 gene nsSNPs, the PolyPhen-2 server was used. The position-specific independent count (PSIC) scores indicate the three possibilities of variants, categorized as benign (scores: 0.0- 0.15), possibly damaging (scores: 0.15 -1.0), and probably damaging (scores: 0.85 - 1.0), have rigorous effects. PolyPhen-2 examines the physical attributes of the wild-type and mutant variants to assess the detrimental probability of a mutation. It employs multiple sequence alignment and a machine learning-based classifier designed for high-throughput NGS data processing. It calculates the variant's PSIC scores and then estimates the difference in PSIC between the mutant and the wild-type. The PSIC score >0.90 is considered a deleterious mutation. Results show that out of 536 nsSNPs, 229 were predicted as benign, having a score less than or equal to 0.15. The possibly damaging effect was predicted for 72 nsSNPs, with a score less than or equal to 1.0. Whereas 235 nsSNPs were predicted as deleterious, having a PSIC score of ~1.0.

To find non-synonymous or indel variants that are predicted to be functionally significant, PROVEAN is helpful for filtering sequence variants. The protein variant is expected to have a "deleterious" effect if the PROVEAN score is equal to or falls below a predetermined threshold, such as -2.5. The variant is predicted to have a "neutral" effect if the PROVEAN score is higher than the threshold. The alignment scores are calculated to correspond to the sequence clusters. Results show that among the 536 nsSNPs, 171 nsSNPs were predicted as deleterious with a score less than -2.5, whereas 230 were predicted to have a neutral effect, where the score is higher than the threshold > -2.5.

Another analysis was performed using SIFT to determine the possibilities of induced missense mutations and naturally occurring nsSNPs. It examines the influence of amino acid position alterations and substitutions on the function of a protein. The SIFT score varies between 0.0 (deleterious) and 1.0 (tolerated). Variants whose scores fall within the range of 0.0−0.05 are deleterious. Harmful effects are more confidently predicted for variants with scores that are close to 0.0. This analysis results in the selection of 163 nsSNPs as deleterious, whereas 195 nsSNPs are predicted as tolerated.

Predictions using I-Mutant 2.0 are made either from the protein structure or, more crucially, from the protein sequence. I-Mutant 2.0 was examined based on the protein sequence, mutational position, and interrelated new residue. In addition, I-Mutant 2.0 was applied to predict the protein stability in terms of free energy, resulting from a single-point mutation in a protein structure or sequence. The predicted free energy change (ΔG) output divides the results into two categories: decreased stability (DDG < 0) and increased stability (DDG > 0). The cross-correlation validation between the predicted observed ΔG values determines the accuracy of I-Mutant results. Out of 536 nsSNPs, a total of 182 nsSNPs were predicted to have either decreased or increased stability, which was observed to be consistent with the results obtained using PolyPhen-2, PROVEAN, and SIFT, as shown in **Table 2**.

PANTHER estimates the probability of a certain altering amino acid non-synonymous coding SNP that will have a functional effect on the protein. It computes the amount of time that a certain amino acid has been present in the pathway leading to the protein of interest. The possibility of a functional effect may increase with the preservation time. To examine the evolutionary preservation, PANTHER-PSEP was applied, which recreates the possible sequences of ancestor proteins at points of the phylogenetic tree, and the natural history of all amino acids can be followed from their present state back

in time to determine how long that condition has been preserved in their ancestors. Hereby, we explain the PSEP tool and evaluate how well it performs on standard criteria for identifying disease-related from neutral variations in human beings. On these standards, PSEP outperforms not just previous tools that use evolutionary conservation but also a number of widely used tools that use several more data sources. As a result, 262 nsSNPs were predicted as probably damaging, having a false rate of approximately 0.2, whereas 66 nsSNPs were predicted as possibly damaging and 124 nsSNPs were predicted as probably benign, whereas the remaining 84 nsSNPs showed no score, counted as an invalid substitution.

Furthermore, SVM-based PhD-SNP was applied to predict possible mutations. It divides mutations into neutral polymorphism, where the desired output is set to 1, or disease-related mutations, where the desired output is set to 0. The threshold for deciding is set at 0.5, and the reliability index (RI) value was evaluated. The sequence profile is computed using an input vector formed from wild-type (WT) and mutant amino acid frequencies, the number of matched sequences, and the conserved score in the substituted site. A PhD-SNP score greater than 0.5 suggests the presence of a disease-causing mutation. Results show 214 nsSNPs as disease-causing mutations, 315 nsSNPs predicted as neutral, and the remaining 7 nsSNPs showed no scores.

Finally, to further affirm the functional diversity of SLC11A1 nsSNPs, a Meta-SNP-based analysis was performed, providing an integrated result of PANTHER, PhD-SNP, SIFT, and SNAP. Meta-SNP is a widely accepted tool for GWAS analysis. It takes single-predictor outputs as input and was trained and evaluated using a 20-fold cross-validation process on the SV-2009 dataset (https://snps.biofold.org/meta-snp/pages/data/SV-2009.txt). The values reported under each prediction should be between 0 and 1, and the scores > 0.5 suggest that the predicted nsSNP is associated with disease. The SV-2009 dataset contains 17,883 disease-related mutations and a similar number of polymorphisms that have been selected randomly. During the cross-validation process, proteins are organized using the blastclust method in the BLAST software, and any variants that belong to an identical cluster of comparable sequences are placed in the same set. Using Meta-SNP, 243 nsSNPs are predicted as disease-associated, 208 nsSNPs were found neutral, whereas 85 nsSNPs showed no scores.

However, the results of Polyphen-2 analysis suggested the damaging mutation impacts of 235 nsSNPs. PROVEAN shows a deleterious mutational effect for 171 nsSNPs, whereas the deleterious mutations estimated by SIFT result in the selection of 163 nsSNPs. I-Mutant was applied to examine the impact of mutants on the stability of protein, which categorized 182 nsSNPs as high-risk mutations. PANTHER-based analysis indicated the damaging effects of 262 nsSNPs. While using PhD-SNP, 214 nsSNPs were predicted to be associated with disease, whereas 243 nsSNPs were predicted as disease-associated by Meta-SNP. Finally, a comparative analysis of applied methods was performed, which provided a consensus result of 11 nsSNPs, having deleterious effects. The disease-associated 11 nsSNPs are enumerated in **Table 2**.

Table 2: Validation of nsSNPs in SLC11A1 gene using PolyPhen-2, PROVEAN, SIFT, I-Mutant, PANTHER, PhD-SNP, and Meta-SNP

Comparative study																			
				PolyPhen 2		Provean		Sift	I - Mutant			Panther		Phd - SNP		Meta-SNP			
SNP ID	Allele	Amino Acid Change	Amino Acid Change	Score	Prediction	Score	Prediction	Score	Prediction	DDG Value (Kcal/mol)	Prediction	Preservation time	Prediction	Pdel	Reliability Index(RI)	Prediction	Reliability Index(RI)	Value	Prediction
rs139480250	G>A	Ala173Thr	A173T	1	Probably damaging	-3.781	Deleterious	0.001	Deleterious	-1.9	Decrease	1629	Probably damaging	0.89	2	Disease	5	0.725	Disease
rs141932707	T>C	Ile40Thr,	I40T	1	Probably damaging	-4.7	Deleterious	0.03	Deleterious	0.1	Increase	3806	Probably damaging	0.89	8	Disease	4	0.707	Disease
rs 145536242	T>C	Leu174Prc	L174P	1	Probably damaging	-6.615	Deleterious	0	Deleterious	-1.24	Decrease	1629	Probably damaging	0.89	8	Disease	6	0.821	Disease
rs 150192588	T>A	Phe188Le	F188L	1	Probably damaging	-5.571	Deleterious	0.002	Deleterious	-1.36	Decrease	1629	Probably damaging	0.89	3	Disease	2	0.632	Disease
rs151164925	C>T	Ser46Leu,	S46L	1	Probably damaging	-5.461	Deleterious	0.006	Deleterious	0.64	Increase	1628	Probably damaging	0.89	2	Disease	3	0.669	Disease
rs 182057473	A>G	Tyr395Cys	Y395C	1	Probably damaging	-8.193	Deleterious	0	Deleterious	-1.95	Decrease	1629	Probably damaging	0.89	9	Disease	7	0.831	Disease
rs 182057473	A>G	Tyr364Cys	Y364C	1	Probably damaging	-7.815	Deleterious	0	Deleterious	-3.73	Decrease	3806	Probably damaging	0.89	7	Disease	7	0.832	Disease
rs201910426	C>T	Arg16Cys,	R16C	1	Probably damaging	-7.313	Deleterious	0	Deleterious	-0.19	Decrease	1628	Probably damaging	0.89	8	Disease	6	0.807	Disease
rs367630718	A>C,G	Tyr94Cys,	Y94C	1	Probably damaging	-7.966	Deleterious	0.022	Deleterious	-2.99	Decrease	1237	Probably damaging	0.85	5	Disease	6	0.813	Disease
rs375775521	G>A	Gly271Ser	G271S	1	Probably damaging	-5.776	Deleterious	0.004	Deleterious	-0.56	Decrease	4200	Probably damaging	0.95	8	Disease	6	0.803	Disease
rs377166486	A>C,G	Asn362Ser	N362S	1	Probably damaging	-4.683	Deleterious	0	Deleterious	-0.89	Decrease	3806	damaging	0.89	9	Disease	4	0.692	Disease

3.3 Structural analysis

The alterations in amino acid sequences by nsSNPs may affect the structure and stability of NRAMP1, thereby increasing the susceptibility to disease. Evaluating the effect of nsSNPs on protein may provide an important clue for determining the impact of a mutation on disease. Several computational studies followed by experimental analyses provided a comprehensive understanding of the biological mechanisms of nsSNPs in a wide range of diseases. Thus, to examine the structural and functional aspects, the three-dimensional structure of human NRAMP1 protein was predicted, selecting the NRAMP1 protein (PDB ID: 5M8K) of E. coleocola as a template. The sequence alignment with the chosen template is shown in **Figure 3A.** The predicted structure quality assessment of human NRAMP1 shows that 91.20 % of residues are in the most favorable region of the Ramachandran plot (RC-plot), 7.60 % of residues are observed in the additional allowed region, whereas no residues are found in the disallowed regions. Based on the nsSNPs analysis, the three-dimensional structures for all 11 deleterious mutants were predicted, and the structural superimposition with wild-type NRAMP1, total energy minimization, and RMSD values were calculated. Further, ASA, Hydrogen-bond energy, and model quality was checked by VADAR. To understand the protein structure-function relationship, the ligand binding site of NRAMP1 was predicted on FT-Site. Using the STRING database, network analysis was performed for the prediction of protein-protein interactions and associated functions.

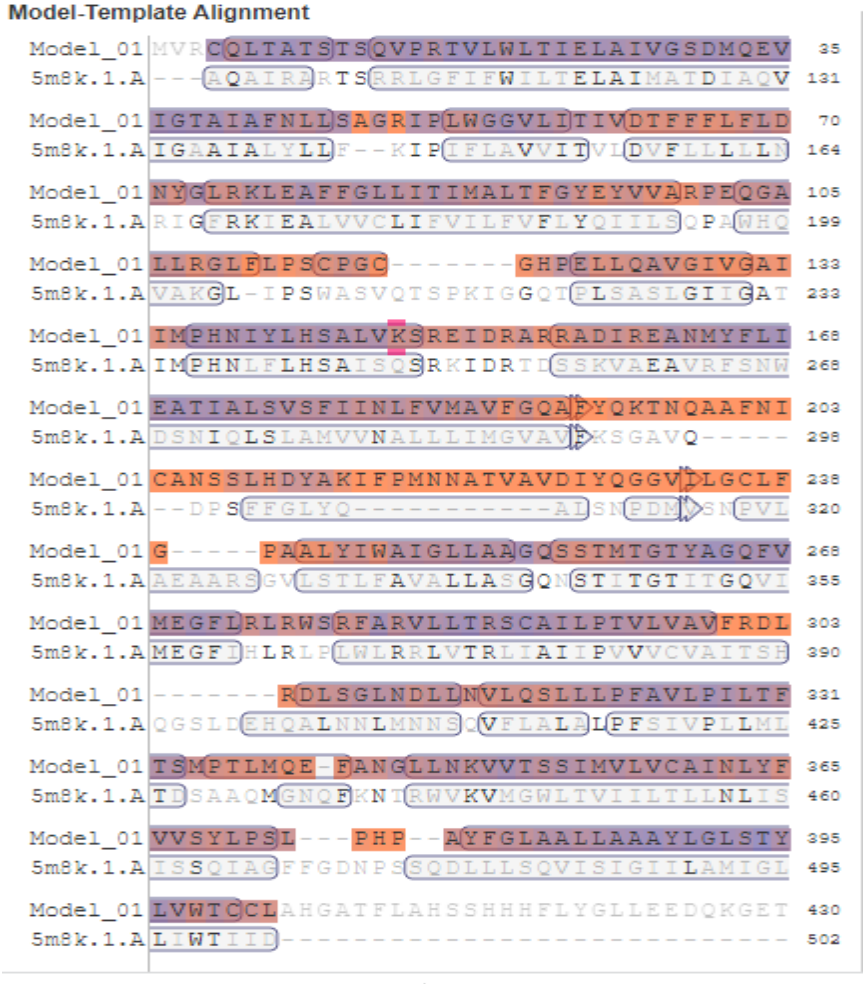

Figure 3A: Sequence alignment of wild-type protein (NRAMP1) with selected template (PDB ID: 5M8K). The overall sequence similarity of NRAMP1 (P49279-2) with template is 99.8 %.

Generation of mutants

Using the three-dimensional structure of human NRAMP1, the structures for the selected deleterious mutants were generated on PyMol. The 3D-structures of NRAMP1 and mutant models are shown in **Figure 3B**. Due to the mutations, changes in the sequence of amino acids may affect the structure, functions, and spatial binding of ligands.

(a) Native Model

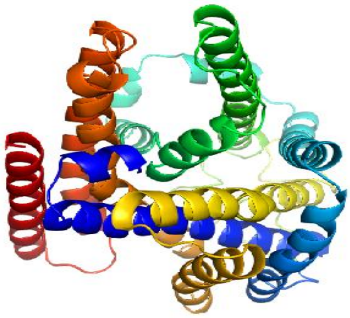

(b) A173T

(c) I40T

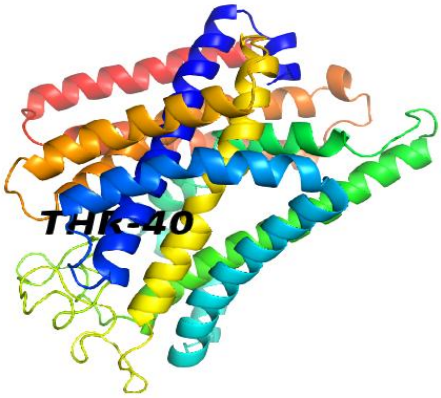

(d) L174P

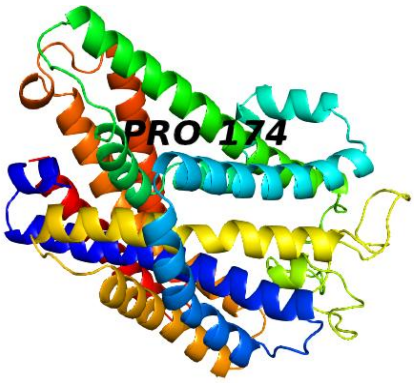

(e) F188L

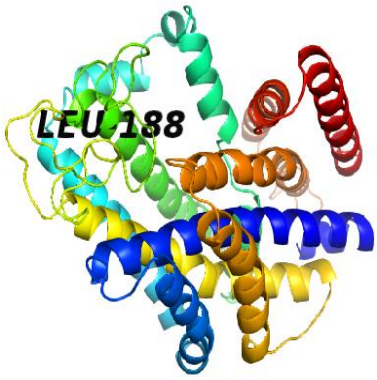

(f) S46L

(g) Y395C

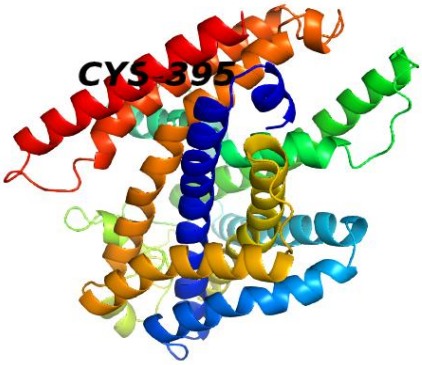

(h) Y364C

(i) R16C

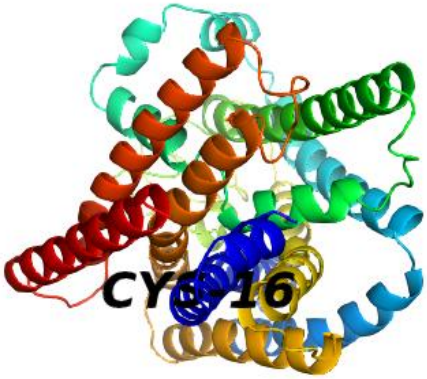

(j) Y94C

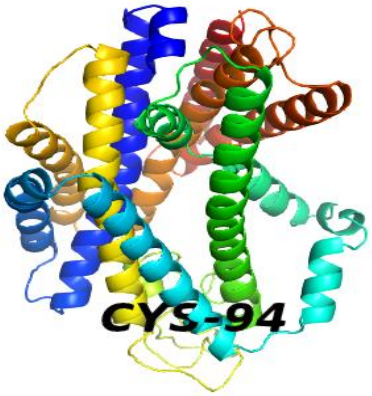

(k) G271S

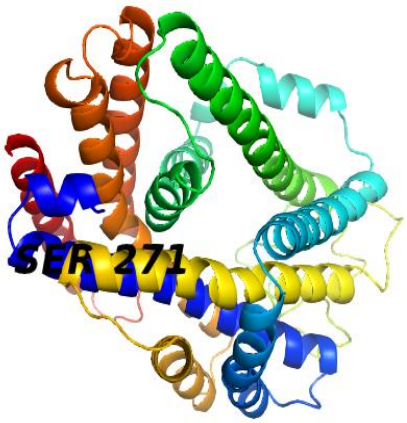

(l) N362S

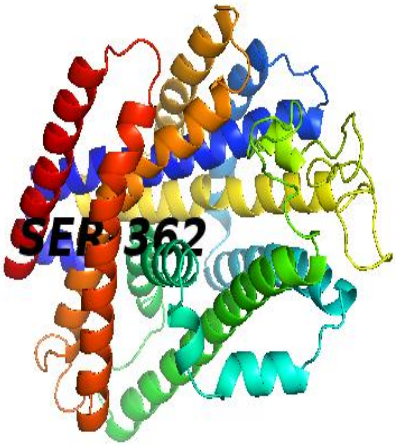

Figure 3B: Three dimensional structures of (a) human NRAMP1 and mutants (b) rs139480250 (Ala173Thr) (c)rs141932707(lle40Thr) (d)rs145536242(Leu174Pro) (e) rs150192588(Phe188Leu) (f)rs151164925(Ser46Leu) (g)rs182057473(Tyr395Cys) (h) rs182057473(Tyr364Cys) (i)rs201910426(Arg16Cys) (j)rs367630718(Tyr94Cys) (k) rs375775521(Gly271Ser) (l) rs377166486(Asn362Ser).

3.4 Energy minimization and RMSD analysis

The comparative analysis of energy minimization of wild-type and mutants show differences of approximately ~1000 KJ/Mol (**Table 3**). The difference in energies indicates less stable structures of mutants as compared to wild-type (WT). The 3D structure of a protein is largely stabilized by the various interactions, polar, non-polar, and Vander Waals

interactions. The mutation of amino acids influences the dynamic stability of proteins, by the loss of molecular interactions results in an increase in entropy. Thus, RMSD values were calculated by superimposing the structures of mutant with WT (**Figure 4, Table 3**). Results show that among the 11 nsSNPs, the structural superimposition with rs182057473 displays a higher RMSD value (1.45 Å), suggesting the more deleterious effect of Tyr395Cys mutation.

(a) A173T

(b) I40T

(c) L174P

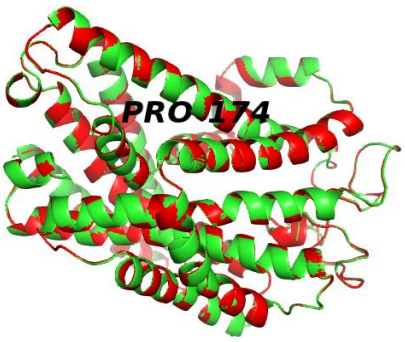

(d) F188L

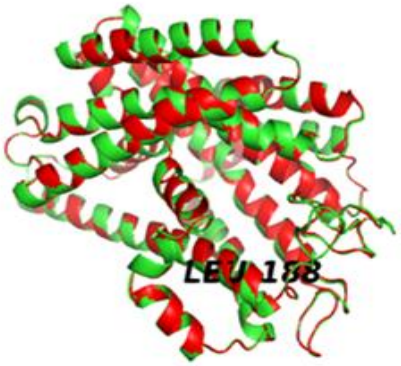

(e) S46L

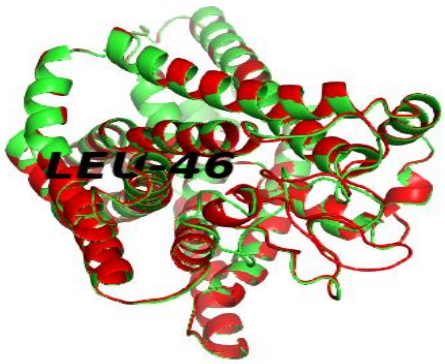

(f) Y395C

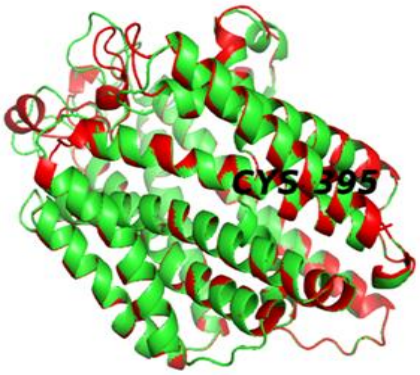

(g) Y364C

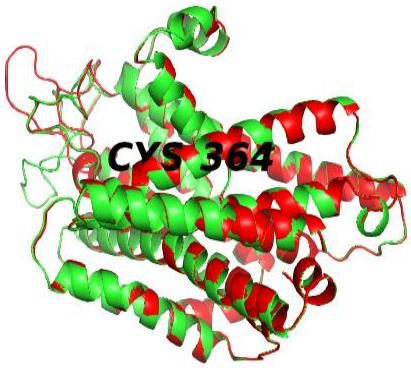

(h) R16C

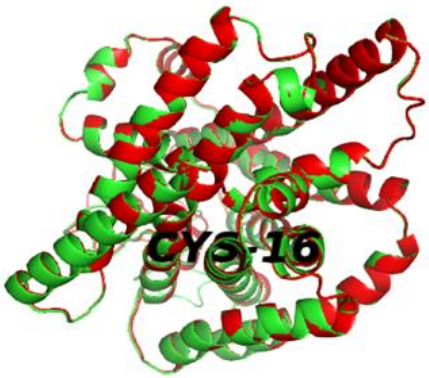

(i) Y94C

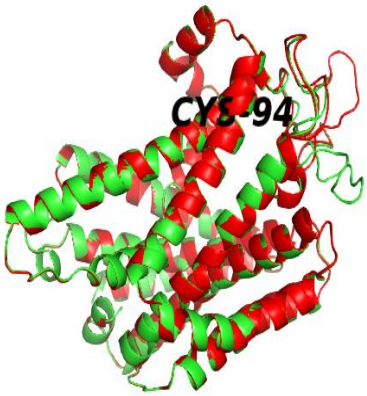

(j) G271S

(k) N362S

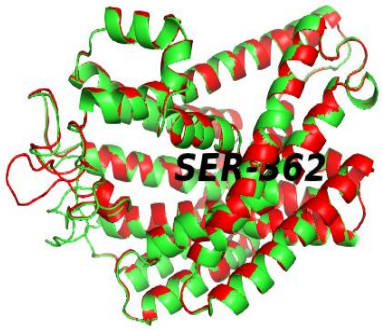

Figure 4: Structural superimposition of WT with nsSNPs.

Table 3: Total energy after minimization of mutant model and RMSD value

			Energy Calculation		RMSD Calculation
Model	Allele Change	Amino acid change	Total Energy(KJ/Mol)		RMSD(Å)
			Before energy minimization	After energy minimization	
Native			-13938.625	-18691.605	
rs139480250	G>A	Ala173Thr, A173T	-12932.424	-18143.021	0.157
rs141932707	T>C	Ile40Thr, I40T	-13801.278	-18613.67	0.055
rs145536242	T>C	Leu174Pro, L174P	-13381.668	-18234.27	0.11
rs150192588	T>A	Phe188Leu, F188L	-12941.581	-18012.076	0.173
rs151164925	C>T	Ser46Leu, S46L	-12440.779	-17670.008	1.132
rs182057473	A>G	Tyr395Cys, Y395C	-13774.973	-18567.096	1.456
rs 182057473	A>G	Tyr364Cys, Y364C	-12493.107	-17706.311	1.132
rs201910426	C>T	Arg16Cys, R16C	-12650.355	-17951.744	1.134
rs367630718	A>C,G	Tyr94Cys, Y94C	-12476.471	-17720.584	1.134
rs375775521	G>A	Gly271Ser, G271S	-13853.552	-18681.996	0.232
rs377166486	A>C,G	Asn362Ser, N362S	-12169.923	-17521.719	1.131

3.5 Estimation of accessible surface area (ASA), H-bond energy, and Model quality

To investigate the structural stabilities of proteins, we also computed the accessible surface area (ASA) and hydrogen bond (H-bond) energy, as shown in **Table 4**. Comparing the ASA values of (WT)native and mutant structures, results show that the overall exposed non-polar ASA of mutants is decreased slightly, except rs151164925(Ser46Leu) and rs377166486(Asn362Ser). However, the total ASA of mutants, i.e., rs145536242(Leu174Pro) and rs375775521(Gly271Ser) observed slightly less as compared to the native protein. Even the exposed polar ASA values of all mutants obtained high as compared to native (3846.9 Å). Whereas the exposed charged ASA results show a marginal high ASA of rs182057473(Tyr395Cys). Remarkably, the hydrophobicity of all mutants and native protein remains consistent indicating the stable structural folds of protein. The deviation of ASA may contemplate the less stable structural dynamics of mutants.

Table 4: Calculation of H-bond energy and accessible surface area (ASA) by VADAR server

			H-bond Energy(KJ/M)		Accessible Surface Area(ASA)				
Model	Allele change	Amino acid change	Native	Mutant	Total ASA	Exposed non-polar ASA	Exposed polar ASA	Exposed charged ASA	% side ASA hydrophobic
Native					22271.8 Å^2	16309.4 Å^2	3846.9 Å^2	2115.4 Å^2	53.56
rs139480250	G>A	Ala173Thr, A173T	-2.2	-2.35	22303.7 Å^2	16180.1 Å^2	3919.4 Å^2	2204.2 Å^2	52.83
rs141932707	T>C	Ile40Thr, I40T	-2.53	-2.7	22288.6 Å^2	16305.0 Å^2	3848.8 Å^2	2134.9 Å^2	53.56
rs 145536242	T>C	Leu174Pro, L174P	-2.85	-2.33	22260.5 Å^2	16176.1 Å^2	3897.8 Å^2	2186.5 Å^2	53
rs150192588	T>A	Phe188Leu, F188L	-2.38	-2.15	22317.8 Å^2	16204.3 Å^2	3909.1 Å^2	2204.5 Å^2	53.08
rs151164925	C>T	Ser46Leu, S46L	-1.33	-1.51	22557.0 Å^2	16315.4 Å^2	4021.5 Å^2	2220.1 Å^2	53.07
rs182057473	A>G	Tyr395Cys, Y395C	-2.09	-2.01	22428.9 Å^2	16256.5 Å^2	3910.0 Å^2	2262.4 Å^2	53.72
rs182057473	A>G	Tyr364Cys, Y364C	-2.01	-2.18	22514.5 Å^2	16292.1 Å^2	4019.1 Å^2	2203.4 Å^2	53.5
rs201910426	C>T	Arg16Cys, R16C	-1.41	-1.62	22399.5 Å^2	16229.0 Å^2	3951.8 Å^2	2218.8 Å^2	53.34
rs367630718	A>C,G	Tyr94Cys, Y94C	-2.27	-2.72	22551.8 Å^2	16280.3 Å^2	4043.9 Å^2	2227.7 Å^2	53.17
rs375775521	G>A	Gly271Ser, G271S	-1.05	-1.46	22196.6 Å^2	16237.5 Å^2	3873.3 Å^2	2085.8 Å^2	53.93
rs377166486	A>C,G	Asn362Ser, N362S	-2.22	-2.75	22536.6 Å^2	16328.8 Å^2	4003.6 Å^2	2204.1 Å^2	53.28

3.6 Ligand Binding Site Prediction

To determine the impact of predicted nsSNPs on the spatial binding of ligands with protein, the active site of SLC11A1 is define by FT-Site. Furthermore, to resolve the basic challenge related to the understanding of the relation between protein structure-function, protein engineering, and drug design, protein binding sites were viewed as hot spot locations, particularly for tiny ligand molecules. With an experimental accuracy of 94% and 97% for the LIGSITE^{CSC} and QSiteFinder sets, FT-Site is a precise computational technique based on the evidence of experiments to identify the highest-ranked ligand binding sites(Ngan et al., n.d.). Based on the analyses, three ligand-binding sites are identified. The residues around the 7Å from the center of active sites are listed in **Table 5**. Out of eleven nsSNPs identified, one nsSNP i.e., rs150192588(Phe188Leu) was found in the first binding site of the protein shown in **Figure and Table 5**. Thus, the final nsSNP rs150192588(Phe188Leu) of SLC11A1 gene can be a potential drug target for the treatment of spinal tuberculosis.

Table 5: Ligand Binding Site Prediction of SLC11A1

Binding Site	Amino acid Residues														
Site select 1	88	92	184	**188**	209	212	246	249	253						
	MET	PHE	VAL	**LEU**	LEU	TYR	TRP	GLY	ALA						
Site select 2	33	37	209	250	253	310									
	GLN	GLY	LEU	LEU	ALA	ASN									
Site select 3	27	30	31	33	81	84	88	135	137	177	180	252	256	260	261
	ILE	SER	ASP	GLN	PHE	LEU	MET	MET	HIS	SER	ILE	ALA	SER	THR	GLY

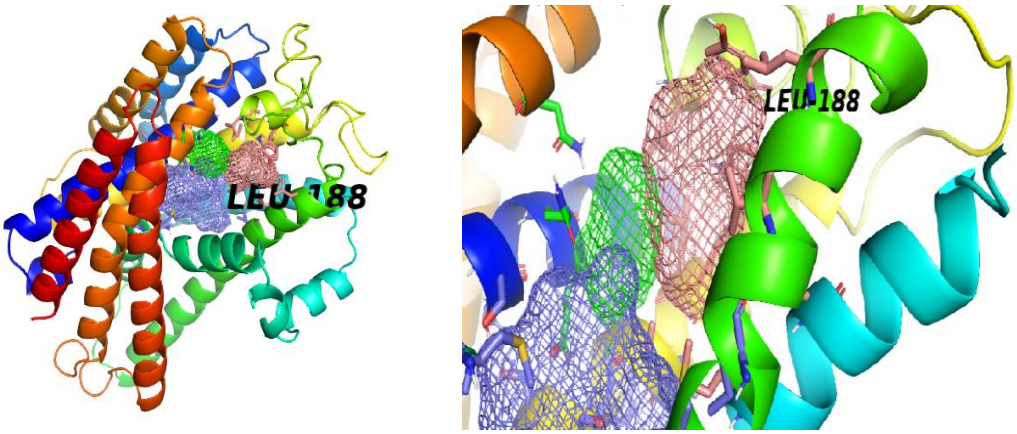

Figure 5: Ligand binding site protein (SLC11A1): The three predicted ligand binding sites are shown in this figure. The 1st ligand binding site is coloured in pink. The 2nd ligand binding site is coloured in green, and the 3rd ligand binding site is coloured in purple where the rs150192588(Phe188Leu) nsSNP is present at the 1st ligand binding site of protein.

3.7 Protein-protein interactions

A typical network analysis of SLC11A1 gene was performed using STRING. Results show the network status of SLC11A1 consisting of 11 number of nodes that represent proteins, and 19 edges representing protein-protein associations. The average node degree value of 3.45 and the average local clustering coefficient of around 0.852, offer a framework for analysing the conserved patterns in the organization of the genome which is shown in **Figure 6**. The protein network analyses of SLC11A1 gene show the functional association with SLC11A2 (Natural resistance-macrophage protein-2). The genes SLC11A1 and SLC11A2, both belonging to NRAMP family, are involved in metal transportation. The SLC11A1 gene is a divalent transition metal (iron and manganese) transporter implicated in iron metabolism and host resistance to some infections whereas SLC11A2 gene along with iron also involve in transportation of other metal ions, e.g., manganese, cobalt, cadmium, nickel, vanadium, and some extent lead also. It is engaged in absorption of iron into duodenal enterocytes, from acidified endosomes into the cytoplasm of erythroid precursor cells and plays a crucial function in hepatic iron buildup and tissue iron distribution.

The solute carrier genes are also involved in metal transportation, SLC40A1 gene is involved in iron export from duodenal epithelial cells as well as iron transfer between maternal and foetal circulation and the gene SLC31A2 is a copper ion transporter, regulates cellular copper ion homeostasis. SLC25A37 plays a vital role in mitochondrial heme and iron-sulfur clusters as an iron importer. SLC34A1 act as phosphate symporter, involved in various functions, including phosphate ion homeostasis, phosphate ion transport, and lead ion response. It is involved in several diseases including fanconi syndrome; chronic kidney disease; inherited hypophosphatemic rickets with hypercalciuria; hypophosphatemic nephrolithiasis/ osteoporosis 1; and nephrolithiasis.

ATP7A gene encodes a transmembrane protein involved in copper transport across membranes. The mutation in this gene leads to X-linked distal spinal muscular atrophy, Menkes disease, and occipital horn syndrome. TTN gene produces a considerable amount of striated muscle protein involved in contractile machinery in muscle cells. Mutations in TTN are linked to familial hypertrophic cardiomyopathy and autoimmune illness scleroderma. FGA gene encodes the alpha subunit of fibrinogen, a coagulation factor and component of blood clots. Several illnesses are caused by mutations in this gene, including dysfibrinogenemia, hypofibrinogenemia, afibrinogenemia, and renal amyloidosis. Alternative splicing generates numerous transcript variants, at least one of which yields a proteolytically processed isoform. HAMP maintains iron homeostasis and mutations in it are characterized by severe iron overload, resulting in cirrhosis, cardiomyopathy, and endocrine failure. SPI1 encodes an ETS-domain transcription factor that regulates gene expression throughout the development of myeloid and B-lymphoid cells and may control target gene alternative splicing, results in distinct isoforms.

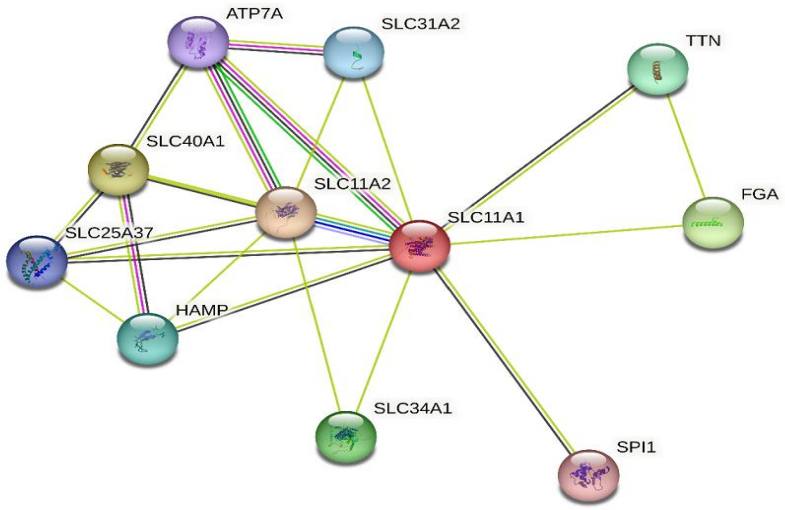

Figure 6: SLC11A1 network analysis. (a) Colour nodes indicates query proteins and first shell of interactors. (b) White nodes indicate second shell of interactors. (c) Empty nodes indicate proteins of unknown 3-dimensional structure. (d) Filled nodes indicates a 3-dimensional structure is known or predicted.

4. CONCLUSION

In conclusion, the present study focuses on the prediction of disease-associated nsSNPs of SLC11A1 gene. A comprehensive analysis of 536 nsSNPs suggests the possible deleterious effects of 11 nsSNPs which may cause STB disease. Herein, we determine the phenotypic variations and protein function connected to the structure-function relationship of the SLC11A1. Out of eleven nsSNP, nsSNP (Phe188Leu) i.e., rs150192588 has been predicted as high risk for STB susceptibility which is located at the active site of SLC11A1 protein, NRAMP1. Identifying the active site residue may be bestowed for the structure-based drug development in therapy of spinal tuberculosis in humans.

Acknowledgements

SS is thankful to the HPC computational facility at Amity Institute of Integrative Sciences & Health (AIISH) department, Amity University Haryana, and Department of Biotechnology Engineering, Parul University Gujarat for data analyses.

Author contributions

SS, RKS and AP designed the work. SS performed experimental work. RKS and AP supervised the study. All authors contributed to data analysis and manuscript preparation. The final version of the manuscript has been approved by all authors.

Competing interests

The authors declare no competing interests.

Abbreviations:

1. **Mtb** – *Mycobacterium tuberculosis*
2. **STB** – *Spinal Tuberculosis*
3. **nsSNP** – *Non-synonymous Single Nucleotide Polymorphism*
4. **SLC11A1** – *Solute Carrier Family 11, Proton-Coupled Divalent Metal Ion Transporter Membrane 1*
5. **NRAMP1** – *Natural Resistance-Associated Macrophage Protein 1*
6. **NCBI** – *National Center for Biotechnology Information*
7. **PolyPhen-2** – *Polymorphism Phenotyping-2*
8. **PSIC** – *Position-Specific Independent Count*
9. **PROVEAN** – *Protein Variation Effect Analyzer*
10. **SIFT** – *Sorting Intolerant From Tolerant*
11. **ProTherm** – *Thermodynamic Database for Proteins and Mutants*
12. **PANTHER** – *Protein Analysis Through Evolutionary Relationships*
13. **HMM** – *Hidden Markov Model*
14. **subPSEC** – *Substitution Position-Specific Evolutionary Conservation*
15. **PhD-SNP** – *Predictor of Human Deleterious Single Nucleotide Polymorphisms*
16. **SVM** – *Support Vector Machine*
17. **Meta-SNP** – *Meta Predictor of Disease-Causing Variants*
18. **GWAS** – *Genome-Wide Association Study*
19. **RI** – *Reliability Index*
20. **RMSD** – *Root-Mean-Square Deviation*
21. **VADAR** – *Volume, Area, Dihedral Angle Reporter*
22. **PDB** – *Protein Data Bank*
23. **WT** – *Wild-Type*
24. **ASA** – *Accessible Surface Area*
25. **STRING** – *Search Tool for the Retrieval of Interacting Proteins*
26. **SLC11A2** – *Solute Carrier Family 11, Proton-Coupled Divalent Metal Ion Transporter Membrane-2*
27. **SLC40A1** – *Solute Carrier Family 40 Member 1*
28. **SLC31A2** – *Solute Carrier Family 31 Member 2*
29. **SLC25A37** – *Solute Carrier Family 25 Member 37*
30. **SLC34A1** – *Solute Carrier Family 34 Member 1*
31. **ATP7A** – *ATPase Copper Transporting Alpha*
32. **TTN** – *Titin*
33. **FGA** – *Fibrinogen Alpha Chain*
34. **HAMP** – *Hepcidin-20*
35. **SPI1** – *Spi-1 Proto-Oncogene*
36. **ETS** – *E26 Transformation–Specific Sequence*

REFERENCES

1. Abd Elhamid Fadlalla Elshaikh, A., Mohamed Gasemelseed, M., Mohamed Osman, M., Ahmed Ibrahim Shokri, S., Othman massad, S., Ebrahim Merghani Fadl, N., Habiballa Ibrahim, A., Shiekh Idris, S., Mohamed Abdalla, M., Ahmed Salih, M., 2016. Computational Analysis of Single Nucleotide Polymorphism (SNPs) in Human GRM4 Gene. American Journal of Biomedical Research 4, 61–73. https://doi.org/10.12691/ajbr-4-3-2
2. Akhoundi, F., Parvaneh, N., Modjtaba, E.B., 2016. In silico analysis of deleterious single nucleotide polymorphisms in human BUB1 mitotic checkpoint serine/threonine kinase B gene. Meta Gene 9, 142–150. https://doi.org/10.1016/j.mgene.2016.05.002
3. Alam, S., Sayem, M., Kamrul Hasan, M., Sharmin, Z., Arif Pavel, M., Faruk Hossain, M., n.d. Prediction of Deleterious Single Nucleotide Polymorphisms in Human p53 Gene. https://doi.org/10.1101/408476
4. Ali Mohamoud, H.S., Manwar Hussain, M.R., El-Harouni, A.A., Shaik, N.A., Qasmi, Z.U., Merican, A.F., Baig, M., Anwar, Y., Asfour, H., Bondagji, N., Al-Aama, J.Y., 2014. First comprehensive in silico analysis of the functional and structural consequences of SNPs in human GalNAc-T1 gene. Comput Math Methods Med 2014. https://doi.org/10.1155/2014/904052
5. Amiri, A., Sabooteh, T., Shahsavar, F., n.d. Relationship between common polymorphisms of NRAMP1 gene and pulmonary tuberculosis in Lorestan LUR population. https://doi.org/10.1101/2022.05.01.22274504

6. Datta, A., Mazumder, M.H.H., Chowdhury, A.S., Hasan, M.A., 2015. Functional and Structural Consequences of Damaging Single Nucleotide Polymorphisms in Human Prostate Cancer Predisposition Gene RNASEL. Biomed Res Int. https://doi.org/10.1155/2015/271458
7. Desai, M., Chauhan, J.B., 2019. Predicting the functional and structural consequences of nsSNPs in human methionine synthase gene using computational tools. Syst Biol Reprod Med 65, 288–300. https://doi.org/10.1080/19396368.2019.1568611
8. Elnasri, A., Al Bkrye, A.M., Khaier, M.A.M., 2018. In Silico Analysis of Non Synonymous SNPs in DHCR7 Gene. American Journal of Bioinformatics Research 8, 12–18. https://doi.org/10.5923/j.bioinformatics.20180801.02
9. Garg, R.K., Somvanshi, D.S., 2011. Spinal tuberculosis: A review. Journal of Spinal Cord Medicine. https://doi.org/10.1179/2045772311Y.0000000023
10. Hussain, M.R.M., Shaik, N.A., Al-Aama, J.Y., Asfour, H.Z., Subhani Khan, F., Masoodi, T.A., Khan, M.A., Shaik, N.S., 2012. In silico analysis of Single Nucleotide Polymorphisms (SNPs) in human BRAF gene. Gene 508, 188–196. https://doi.org/10.1016/j.gene.2012.07.014
11. Jin, J., Sun, L., Jiao, W., Zhao, S., Li, H., Guan, X., Jiao, A., Jiang, Z., Shen, A., 2009. SLC11A1 (Formerly NRAMP1) gene polymorphisms associated with pediatric tuberculosis in China. Clinical Infectious Diseases 48, 733–738. https://doi.org/10.1086/597034
12. Li, T., Wang, L., Guo, C., Zhang, H., Xu, P., Liu, S., Hu, X., Gao, Q., 2022. Polymorphisms of SLC11A1(NRAMP1) rs17235409 associated with and susceptibility to spinal tuberculosis in a southern Han Chinese population. Infection, Genetics and Evolution 98. https://doi.org/10.1016/j.meegid.2021.105202
13. Ngan, C.-H., Hall, D., Zerbe, B., Grove, L.E., Kozakov, D., Vajda, S., n.d. FTSite: High accuracy detection of ligand binding sites on unbound protein structures.
14. Patel, S.M., Koringa, P.G., Reddy, B.B., Nathani, N.M., Joshi, C.G., 2015. In silico analysis of consequences of non-synonymous SNPs of Slc11a2 gene in Indian bovines. Genom Data 5, 72–79. https://doi.org/10.1016/j.gdata.2015.05.015
15. Rajasekaran, R., Sudandiradoss, C., Doss, C.G.P., Sethumadhavan, R., 2007. Identification and in silico analysis of functional SNPs of the BRCA1 gene. Genomics 90, 447–452. https://doi.org/10.1016/j.ygeno.2007.07.004
16. Rasouli, M.R., Mirkoohi, M., Vaccaro, A.R., Yarandi, K.K., Rahimi-Movaghar, V., 2012. Spinal tuberculosis: Diagnosis and management. Asian Spine J. https://doi.org/10.4184/asj.2012.6.4.294
17. Saleh, M.A., Solayman, M., Paul, S., Saha, M., Khalil, M.I., Gan, S.H., 2016. Impacts of Non-synonymous Single Nucleotide Polymorphisms of Adiponectin Receptor 1 Gene on Corresponding Protein Stability: A Computational Approach. Biomed Res Int 2016. https://doi.org/10.1155/2016/9142190